

NanoCommunication-based Impermeable Region Mapping for Oil Reservoir Exploration

Liuyi Jin
Texas A&M University
College Station, TX, USA
liuyi@tamu.edu

Zhipei Yan
Texas A&M University
College Station, TX, USA
yanzp@tamu.edu

Lihua Zuo
Texas A&M University-Kingsville
Kingsville, TX, USA
lihuazuo@gmail.com

Radu Stoleru
Texas A&M University
College Station, TX, USA
stoleru@tamu.edu

ABSTRACT

Oil continues to play a significant role in providing worldwide energy. Impermeable zones (i.e., underground areas that allow only few hydrocarbons-collecting fluids, to pass through) can cause significant challenges during the drilling and oil production periods. The problem of mapping an impermeable area has been investigated mainly using seismic sensors deployed on the Earth surface. The existing solutions continue to be imprecise. In this paper we propose a solution that employs nanodevices enabled with wireless THz communication capabilities. The nanodevices are deployed underground and collected as part of oil exploration and recovery. Wireless connectivity among nanodevices is used for mapping underground flow propagation paths, and implicitly, impermeable areas. Since the deployment underground of nanodevices is costly, in this paper we aim to reduce the number of insertion and collection/production wells. Through simulations, we show that our proposed solution achieves good accuracy in mapping impermeable zones, with a reduced cost.

CCS CONCEPTS

• **Computing methodologies** → **Modeling and simulation**; • **Theory of computation** → *Mathematical optimization*.

KEYWORDS

Nanonetworks, Streamline Simulation, Impermeable Area Characterization

ACM Reference Format:

Liuyi Jin, Lihua Zuo, Zhipei Yan, and Radu Stoleru. 2019. NanoCommunication-based Impermeable Region Mapping for Oil Reservoir Exploration. In *The Sixth Annual ACM International Conference on Nanoscale Computing and Communication (NANOCOM '19)*,

Permission to make digital or hard copies of all or part of this work for personal or classroom use is granted without fee provided that copies are not made or distributed for profit or commercial advantage and that copies bear this notice and the full citation on the first page. Copyrights for components of this work owned by others than ACM must be honored. Abstracting with credit is permitted. To copy otherwise, or republish, to post on servers or to redistribute to lists, requires prior specific permission and/or a fee. Request permissions from permissions@acm.org.

NANOCOM '19, September 25–27, 2019, Dublin, Ireland

© 2019 Association for Computing Machinery.

ACM ISBN 978-1-4503-6897-1/19/09...\$15.00

<https://doi.org/10.1145/3345312.3345487>

September 25–27, 2019, Dublin, Ireland. ACM, New York, NY, USA, 7 pages. <https://doi.org/10.1145/3345312.3345487>

1 INTRODUCTION

Energy requirements are expected to increase 1.5 times in the next two decades [16]. Underground Reservoirs (UR), e.g., oil & gas, geothermal, form the majority of energy resources available and are anticipated to remain so to meet the growing energy needs. There is a need to improve the efficiency and cost of extracting energy resources from UR. Among all techniques, *reservoir characterization* (e.g., chemical/physical properties characterization, spatial geometry characterization) plays an important role in determining the reservoir exploration schemes, which further determine the resources extraction efficiency and ultimate recovery. Traditional reservoir characterization techniques provide information about spatial distribution and rock and fluid properties which can be used to build three-dimensional (3D) geologic and dynamic fluid flow models [21]. More recently, 4D seismic technologies have been proposed to track underground fluid movement with sufficient density contrast [22]. These solutions are costly and inaccurate.

Impermeable area detection and characterization is a key part of reservoir characterization. The research in this field dates back to 1987 by Britto and Sageev [5]. They found that the presence of an impermeable region causes the pressure response to deviate from the homogeneous line source response, and the particular deviation indicates that the reservoir is heterogeneous. By transient pressure analysis, Nestor and Heber [17] introduced a new method to detect linear impermeable barriers. The pressure change was analyzed to estimate the distance between the well and the barrier by using the type curve matching technique. More recently, Søndergaard and Auken [24] proposed the idea to map a large scale groundwater through integrated application of geophysics, drillings, logs and geochemistry. They aimed to get a well described picture of the aquifer with respect to localization, distribution, extension, interconnection, etc. To detect an impermeable area, well testing is the only technique that can be used, which generates imprecise picture of the underground impermeable region geometry. Also, neither transient analysis nor integrated data analysis provide real time underground information before actual production.

THz-based nanocommunication network and relevant technology has made much progresses. In [6], Nishtha proposes a THz-based network architecture. This architecture focuses on nanoscale communication amongst collection of nano-devices inside human skin. These nano-devices then communicate with macroscale devices including mobile phones and laptops through THz channel. In this way, the information is retrieved for real-time monitoring of human health. In this paper we also leverage relevant advances in nanotechnology and present an exploration technique to map the impermeable regions of URs as a first step towards optimizing the number of locations of exploration wells. We envision a system that can map, analyze, and optimize the operation of UR exploration. In this paper, nanodevices are employed to detect and map impermeable areas. They are injected into the reservoir via injection wells. After injection, the nanodevices flow through porous media (a nanodevice flows along certain - called *streamline* path all the way to the production wells under the influence of pressure difference), and are finally collected at production wells. During this process, nanodevices communicate wirelessly (THz) among themselves. The nanodevices connectivity data is gathered and used to provide comprehensive information about the reservoirs.

The diameter of nanodevices' flow path in UR is in nanoscale. This requires their geometric size to also be in nanoscale. In such a case, a THz on scheme becomes an obvious choice for our work. In this paper, we make the following contributions:

- We propose, for the first time, the idea of underground oil exploration through nanodevices equipped with wireless communication capabilities
- We formulate the problem of optimal impermeable area mapping, as a minimization on the number of insertion/production oil wells.
- Our simulations results show that an accurate mapping of impermeable areas is possible even with simple communication capabilities.
- We propose ideas for future research that employ more sophisticated cyber-physical components for sensing and communication techniques aimed at improved performance.

This paper is structured as follows: Section 2 reviews background material and state of the art solutions for reservoir characterization. Section 3 gives the system model and formulates the research problem. Our proposed solution is presented in Section 4 and the corresponding performance evaluation results in Section 5, respectively. Finally, we conclude this work in Section 6 and provide directions for future research.

2 STATE OF THE ART AND BACKGROUND

In the area of underground reservoir geometry characterization, hydraulic fractures characterization and monitoring are gaining worldwide attention. Current technology in hydraulic fracturing includes the method to characterize the fracture geometry (e.g., direction, length, aperture, height, plane angles,

and propagation history). In Quirein *et al.* [20], the fundamentals and workflow of microseismic fracture monitoring techniques are introduced. Two wells, one for hydraulic fracturing treatment and one for monitoring, are employed to monitor the fracture. The geophones installed on the monitoring well will process the moveout and the differences in time between P - and S - waves to compute the distance from a monitoring well to the origin of a microseismic event.

Guo [10] proposed a new self-contained micro wireless sensor network framework based on the Magnetic Induction (MI) techniques. He proposed the coiled antenna. The micro coiled antenna is used to realize the wireless communication by generating a magnetic field. The MI technique is also used to power the micro sensor nodes. He validated this framework through theoretical deductions and simulation software. However, the high cost of realizing Guo's framework set back further implementations. Also, the realization of this framework still does not provide sufficient in-situ underground data.

In petroleum engineering, once the reservoir simulation is performed, the streamline simulation is a useful technique to identify the reservoir sections where the most complex flow paths occur for a particular well architecture [8, 26, 27]. In 1988, Pollock [19] proposed a method to compute the streamline trajectory and time of flight (ToF) for cells in regular rectangular shape. Cordes and Kinzelbach [7] generalized Pollock's method to deal with more complex geometries. Simplified versions were further extended by Jimenez *et al.* [12] and Datta-Gupta and King [8]. In the simplified version, the pseudo ToF in corner-point cells is introduced, which is given by Zuo *et al.* [27].

Recently, advances in nanotechnology have triggered a promising set of solutions to explore URs. Nanotechnology has enabled the creation of nanoparticles and "smart fluids" that can vary the surface properties of oil, such as viscosity, wettability, etc. [11, 13–15]. In oil&gas exploration, "smart fluids" can separate oil and water (downhole separation) and for geothermal exploration, they can enhance thermal conductivity [1]. As the technology matures, nanoparticles are expected to become increasingly sophisticated with communication and computation capabilities. This paper builds also on work by Suresh [25], Gong [9] and Ortiz-Lopez [18]. They developed integrated distributed monitoring systems to address the event detection and localization problems in water distribution systems and in drug delivery system for targeted drug delivery.

Despite the aforementioned advances in petroleum engineering, nanomaterials and cyber-physical systems, the problem of accurate mapping of an underground impermeable area remains an open problem, due primarily to the lack of "in-situ" information (e.g., sensors deployed underground).

3 PRELIMINARIES AND PROBLEM FORMULATION

Before we formulate the problem of impermeable region mapping for oil reservoirs, we present the behavior of a nanodevice in the system through a mobility model and a communication

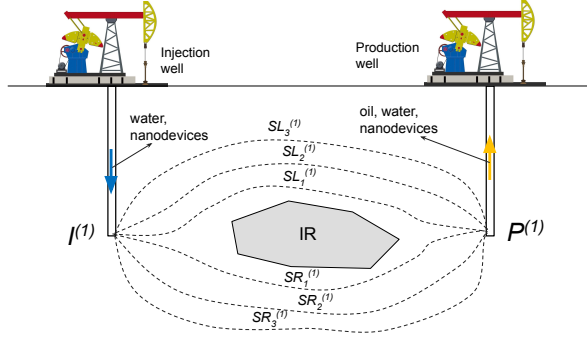


Figure 1: Impermeable Region (IR) mapping in oil exploration using one pair of wells, $I^{(1)}$ and $P^{(1)}$. Nanodevices inserted at $I^{(1)}$ follow streamline paths $SL_i^{(1)}$ or $SR_j^{(1)}$ until they are collected at $P^{(1)}$.

model. Nanodevices, capable of wireless communication using a THz radio [3], are injected into the reservoir through injection wells. Each nanodevice is a receiver and transmitter and flows along a streamline. Nanodevices transmit beacons periodically and record the received signal strength indicator (RSSI) values from other nanodevices. When nanodevices are retrieved from production wells, the RSSI data stored in each receiver is used for interpreting the underground impermeable area geometry.

3.1 System Model

We consider a 2D physical area to be explored for oil as shown in Figure 1. The exploration is performed by drilling wells. Wells can be either for “injection” $\{I^{(k)} | 1 \leq k \leq n\}$ or for “production” $\{P^{(k)} | 1 \leq k \leq m\}$. In injection wells, water, and nanodevices are inserted. These flow through the oil reservoir. Oil, water and nanodevices are collected from production wells.

3.1.1 Mobility Model. For a well pair, there are multiple streamlines between the injection and the production wells. We choose a single streamline for analysis. We deploy nanodevices at a fixed rate, assume there are always $N^{(k)}$ nanodevices along the chosen streamline, defined as $\{n_1^{(k)}, n_2^{(k)}, \dots, n_{N^{(k)}}^{(k)}\}$. It is important to note here that every operation during the impermeable region mapping procedure consists of exactly one injection and one production well. If other wells will be available, they will remain closed temporarily for the sake of independent operation assumption. Note that the superscript does not refer to the exponentiation operation, and is enclosed in brackets to show the difference.

Nanodevices deployed at $I^{(k)}$ traverse streamlines along two distinct sides of an impermeable region IR from the injection well, as shown in Figure 1. Let $\mathcal{SL}^{(k)} = \{SL_i^{(k)}, i \in \mathbb{N}\}$ be the set of streamlines on the “left” side (pick arbitrary side as the left, the other as the right) of the impermeable region and $\mathcal{SR}^{(k)} = \{SR_i^{(k)}, i \in \mathbb{N}\}$ be the set of streamlines on the right side. All streamlines start from injection $I^{(k)}$ and merge at production $P^{(k)}$.

3.1.2 Communication Model. In [4], Akyildiz discussed two propagation models for nanocommunication networks: molecular communication and nano-electromagnetic communication. In this paper, we assume nanodevices are capable of nano-electromagnetic communication. They have THz-based radios capable of transmitting a signal and detecting the RSSI sent from other nanodevices. For the particular oil reservoir application in this paper, the RSSI is dependent on the distance and propagation medium between two nanodevices.

In [2, 3], channel modeling for electromagnetic (EM) wave propagation was implemented in fractures of oil reservoirs. By introducing the propagation medium including crude oil, water, carbon dioxide, soil, the propagation is numerically calculated. In this paper, we adopted the propagation model introduced in [2, 3] except that carbon dioxide is not considered since we are working with conventional reservoir exploration with only water injection for enhancing oil recovery.

For a pair of nanodevices $n_i^{(k)}$ and $n_j^{(k)}$, let $n_i^{(k)}$ be the transmitter and $n_j^{(k)}$ be the receiver without loss of generality. Let $d(n_i^{(k)}, n_j^{(k)})$ be the Euclidean distance between $n_i^{(k)}$ and $n_j^{(k)}$ at some time t . We define the attenuation of the nanodevice transmission using the following pathloss model [3]:

$$\begin{aligned}
 PL(n_i^{(k)}, n_j^{(k)}) &= PL_{spread} + PL_{abs}^{water} + PL_{abs}^{oil} + PL_{abs}^{soil} \\
 &= 20 \log_{10} \left(\frac{4\pi \cdot f \cdot d(n_i^{(k)}, n_j^{(k)})}{c} \right) \\
 &+ k_{water}(f) \cdot d(n_i^{(k)}, n_j^{(k)}) \cdot 10 \log_{10}(e) \\
 &+ k_{oil}(f) \cdot d(n_i^{(k)}, n_j^{(k)}) \cdot 10 \log_{10}(e) \\
 &+ 20 \log(\beta) + 8.69\alpha d(n_i^{(k)}, n_j^{(k)})
 \end{aligned} \tag{1}$$

where PL_{spread} , PL_{abs}^{water} , PL_{abs}^{oil} , PL_{abs}^{soil} are the spread path loss, water absorption path loss, oil absorption path loss and soil absorption path loss, respectively. $PL(n_i^{(k)}, n_j^{(k)})$ is the path loss in decibels during the beacon propagation from $n_i^{(k)}$ to $n_j^{(k)}$ at time t . f is the operating frequency and k_{water} and k_{oil} are the absorption coefficients. α and β are dependent on the dielectric properties of soil, c is the light velocity in vacuum.

As nanodevices move through the streamlines, they record RSSI for all nanodevices in their range of communication. CR is defined as the maximum distance between a nanodevice transmitter n_i and nanodevice receiver n_j such that the receiver can decode the data transmitted by the sender at transmit power P_s . The ability of a nanodevice to decode data is determined by a received power threshold P_{thresh} . If $d(n_i^{(k)}, n_j^{(k)}) < CR$, then $P_r(n_i^{(k)}, n_j^{(k)}) > P_{thresh}$.

As nanodevices split into streamlines $\mathcal{SL}^{(k)}$ and $\mathcal{SR}^{(k)}$, the nanodevices traversing through each set are within CR of each other, but nanodevices in $\mathcal{SL}^{(k)}$ are not within CR of nanodevices in $\mathcal{SR}^{(k)}$ and vice-versa. Note here that we

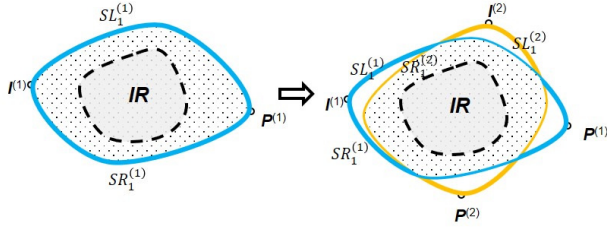


Figure 2: Impermeable Region (solid shaded) geometry characterization through two pairs of insertion and production wells. As shown, using more insertion-production well pairs allows for more accurate mapping.

can set P_{thresh} to a suitable value for this condition to hold, assuming a large enough impermeable region.

In this paper, we make the following simplifying assumptions:

- All streamlines are independent so we choose one streamline as a representative. All nanodevices discussed here are on the chosen streamline.
- The CR of nanodevices is an adjustable parameter. So we assume CR is large enough s.t two sequential nanodevices are always within CR .
- During each test period, exactly one pair of $I^{(k)}$ and $P^{(k)}$ are active. All other injection and production wells, if available, are assumed to be inactive. Each test is assumed to be independent of the others.
- The nanodevices have the size (nano-scale) and form factor to traverse a streamline freely.
- The coarse location of the underground impermeable area is within the loops formed by the two sets of streamlines.

3.2 Impermeable Area Geometry Characterization Problem

The main object of this work is to characterize the geometry of the unknown impermeable region, including the location and the shape. The only input data we can use for the detection are the streamlines between each pair of injection well and production well. A simple fact is that the impermeable region is always inside an arbitrary loop formed by one streamline from \mathcal{SL} and one streamline from \mathcal{SR} like Figure 2. Then the intersection of arbitrary many of such loops still contains the impermeable region. This fact indicates that if we compute the intersection of more and more such loops formed by two streamlines, the intersected area of the loops can be closer and closer to the impermeable region.

An ideal solution to this problem should be: for each pair of injection and production wells, we pick out the streamline loop that wraps the impermeable region the “tightest” and collect all such loops and use the intersection as the prediction of the impermeable region. However, there are two difficulties of this ideal solution. One is that increasing the number of pairs of the injection and production wells or the density of

nanodevices will significantly increase the cost (approx. \$500 per meter of well depth). The other one is that the shape of the streamline is hard to compute. What we can exactly know is only the length of each single streamline.

Based on these two difficulties, we try to approximate the ideal solution with fewer pairs of wells for our impermeable detection scheme. Since the shape of streamline is hard to get, for each well pair $(I^{(k)}, P^{(k)})$, in each streamline set $\mathcal{SL}^{(k)}$ and $\mathcal{SR}^{(k)}$, we chose the shortest streamline. When end points are fixed, the shorter length usually leads to a less twisted streamline shape. We simply use the circular arc which starts and ends at $\{I^{(k)}, P^{(k)}\}$ with the length of the shortest streamline to estimate the real streamline. We denote the region surrounded by the two circular arcs as S_k . Then for the pairs of wells $\{I^{(k)}, P^{(k)}\}_{k=1}^{+\infty}$, we obtain a series of 2D regions $\{S_k\}_{k=1}^{+\infty}$. We define the intersection of first k regions as:

$$S_{\cap}^{(k)} = \bigcap_{i=1}^k S_i. \quad (2)$$

Notice

$$S_{\cap}^{(1)} \supseteq S_{\cap}^{(2)} \supseteq \dots \supseteq S_{\cap}^{(k)} \supseteq \dots$$

Like a positive decreasing series must have a lower limit, the shape series of $S_{\cap}^{(k)}$ has a lower limit.

$$S_{best} = \lim_{k \rightarrow \infty} S_{\cap}^{(k)} = \bigcap_{k=1}^{+\infty} S_{\cap}^{(k)} \quad (3)$$

The S_{best} is the best estimation of the ground truth we can get in this method, though in most cases S_{best} can't be the same as ground truth because S_{best} is always convex in our method, while the ground truth is not. And equation (3) indicates this intersection method can always converge.

The problem in this paper can be formulated as we want to find the smallest k s.t. the current intersection is close enough to the best result we can get:

$$\min_k \{k \mid |S_{\cap}^{(k)} - S_{best}| < \epsilon\}$$

Since S_{best} is impossible to compute, we weaken the problem as:

$$\min_k \{k \mid \frac{|S_{\cap}^{(k)} - S_{\cap}^{(k-1)}|}{|S_{\cap}^{(k)}|} < \epsilon\} \quad (4)$$

Since all estimated regions S_k are independent of k , the optimization problem is how we to choose the location of the well pairs so that $S_{\cap}^{(k)}$ can converge to S_{best} faster. Figure 3 shows an example of our intersection method. Given a square shape impermeable region ABCD, we uniformly deploy 16 wells along a circle containing the impermeable region. We use antipodal wells as a pair of injection and production $\{I^i, P^i\}_{i=1}^8$. Then we use the method above to compute a spindle region S_k formed by two arcs according to $\{I^k, P^k\}$. Then we have 8 regions containing the impermeable. Figure 4 shows the plot of the area of $S_{\cap}^{(k)}$ for k from 1 to 8. We can see that the intersection area reduces quickly in size initially, then the size reduction slows down. This leads to answering the problem: how we can choose the location of the i -th pair of wells so that $S_{\cap}^{(k)}$ converges faster. Since all streamline testing for each

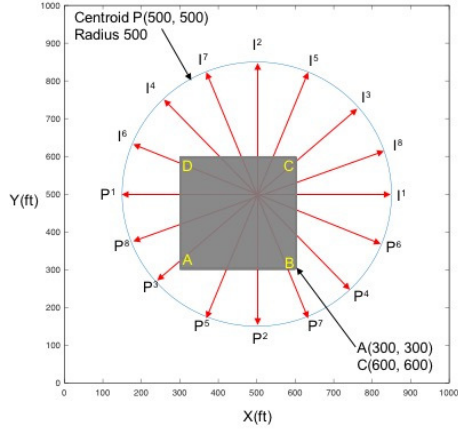


Figure 3: Theoretical analysis for mapping a square impermeable area (shaded rectangle ABCD), using 8 pairs of wells $I^{(1)} \dots I^{(8)}$ and $P^{(1)} \dots P^{(8)}$.

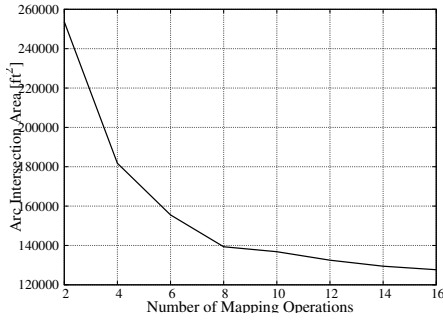


Figure 4: Intersection area decreases as the number of well pairs increases, for the scenario shown in Figure 3.

pair of injection and production are independent, so we can use the result of $S_{\cap}^{(k)}$ to decide the next $\{I^{k+1}, P^{k+1}\}$.

4 PROPOSED SOLUTION

Equation 4 depicts a minimization problem. We want to minimize the total number of mapping operation K to satisfy $\frac{|S_{\cap}^{(k)} - S_{\cap}^{(k-1)}|}{|S_{\cap}^{(k)}|} < \epsilon$ where ϵ is given and $K > 1$. We proposed Algorithm 1 to solve this minimization problem. As we get $S_{\cap}^{(1)}$ after adding first well pair, we repeatedly use *ComputeDiameter*, *FindNextWellPair* and *AddOneMorePair* sequentially until the stopping criterion is reached. Given $(S_{\cap}^{(k)})$, *ComputeDiameter* returns the two end points of the diameter for $(S_{\cap}^{(k)})$. *FindNextWellPair* takes the diameter and computes its perpendicular bisector line, which intersects with circle in Figure 3 at 2 points representing the injection and production well points for next mapping operation. Algorithm 1 comes from the idea that injection and production along perpendicular bisector orientation can maximize the likelihood to chunk greater area

Algorithm 1: Find Optimal Number of Mappings

Input : $I_1(x_I, y_I)$ - coordinates of initial injection well;
 $P_1(x_P, y_P)$ - coordinates of initial production well;
 ϵ - stopping criterion;
Output: Total Number of Mapping K

- 1 $S_{\cap}^{(1)} = \text{AddOneMorePair}(I_1, P_1)$;
- 2 $k = 2$;
- 3 **REPEAT** $[E_{k1}, E_{k2}] = \text{ComputeDiameter}(S_{\cap}^{(k)})$;
- 4 $[I_{k+1}, P_{k+1}] = \text{FindNextWellPair}(E_{k1}, E_{k2})$;
- 5 $S_{\cap}^{(k+2)} = \text{AddOneMorePair}(I_{k+1}, P_{k+1})$;
- 6 $k = k + 2$;
- 7 **UNTIL** $\left(\frac{S_{\cap}^{(k+2)} - S_{\cap}^{(k)}}{S_{\cap}^{(k+2)}} < \epsilon \right)$

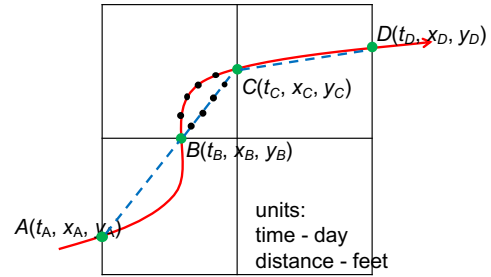


Figure 5: Real streamline (red solid curve) and its approximated counterpart (blue dashed straight line). Black dots represent nanodevices moving along streamlines.

from current $(S_{\cap}^{(k)})$. In another word, we are maximizing the “chunkable” area from previous $(S_{\cap}^{(k-1)})$ in each iteration. In this way, the number of mapping operations can be minimized. We want to point out that, in *AddOneMorePair*, I_k and P_k are used interchangeably to perform 2 consecutive mapping operation.

5 SIMULATIONS AND PERFORMANCE EVALUATION

In this paper, streamlines are numerically generated in two phases. In the first phase, the Eclipse reservoir simulator [23] produces the pressure and velocity distributions. In the second phase, the pressure and velocity distributions are used for obtaining the streamlines, based on work by Pollock and others [8, 19, 27]. The parameters we use in Eclipse are presented in Table 1. As shown, we consider a 2D, 1000ft \times 1000ft area, as in Figure 3. Importantly, the resolution of the simulator is limited (in our scenario we set it to 1ft), which is inadequate for our nanoscale communication scenario. The limitation in the resolution of the simulator is due to the fact that the physics it is based on applies only to macro-environments, not nano-environments.

Table 1: Eclipse Reservoir Simulation Model Parameters

Dimensions (ft)	Grid Size(ft)	Porosity (%)	Permeability (mD)	Injection (bbls/day)	Production (bbls/day)
1000×1000×1	1×1×1	20	10	1000	1000

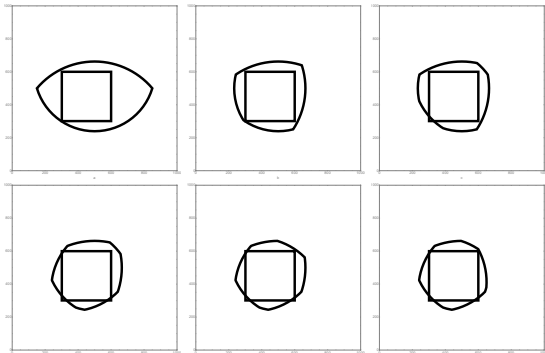
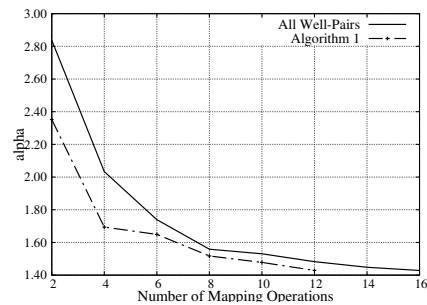


Figure 6: Mappings of a square impermeable area by an increasing number of well-pairs, as decided by Algorithm 1. As shown, the area enclosed by arcs becomes smaller from (a) to (f).

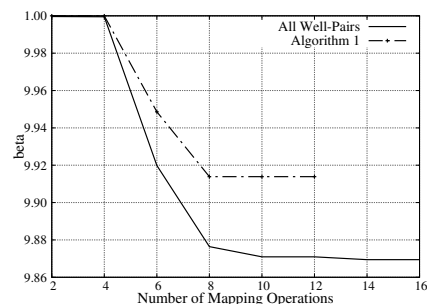
To cope with the limitations in the simulator’s resolution, we present here our approach. In Figure 5, the solid red curve denotes a “real streamline” intersecting 3 simulation grids sequentially at 4 points: A, B, C, D . A “real streamline”, however, can not be exactly obtained. The only information that can be obtained from the simulator are the four points A, B, C, D . To account for nanodevices movement and to obtain $d(n_i, n_j)$ we first approximate each streamline segment within a grid with a straight line segment (i.e., blue line of dashes) directly connecting two points on the grid faces. Second, we evenly divide each straight line segment into smaller segments. It can be seen that the dashed blue line segment BC is divided into several smaller segments by the evenly placed black dots. Those dots can be regarded as the evenly injected nanodevices flowing along the red curvy streamline path. Through even division of the dashed blue straight line segment BC , the space and time are discretized into smaller scale to accommodate nanodevices communication. If the sampling resolution is high enough, the straight line segment can be discretized at nanoscale. Then it is reasonable to assume we can obtain the RSSI between nanodevices n_i and n_j flowing on this segment, and, implicitly, the actual distance between 2 sequential nanodevices n_i and n_j (by employing the pathloss model presented in Equation 1). Ultimately, the total length of the streamline can be obtained by adding all smaller trace lengths between sequential nanodevices.

5.1 Performance Evaluation

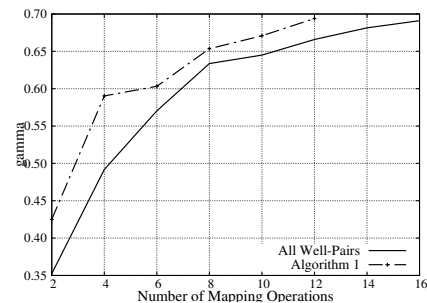
In this section we present the evaluation of our proposed Algorithm 1. First, we present qualitative results, showing the contribution of additional well-pairs (as decided by Algorithm 1) to the accuracy of the impermeable area mapping. Second,



(a)



(b)



(c)

Figure 7: Performance evaluation of Algorithm 1 and comparison with the “All Well-Pair Scheme” for the three proposed metrics: a) $\alpha(k)$; b) $\beta(k)$; and c) $\gamma(k)$.

we present quantitative results for the accuracy of our Algorithm 1, when compared with the optimal solution that considers all well-pairs (and, thus, called “All Well-Pairs”).

For our simulations, we consider a scenario as shown in Figure 3. In a 2D area, 1000ft × 100ft, an impermeable square area (300ft × 300ft) is present.

The qualitative results of our simulation are depicted in Figure 6(a-f). In Figure 6(a) a single well-pair is used and in each subsequent figure (b-f) a new well-pair is used for refining the mapping of underground impermeable area. As shown, our

Algorithm 1 decision of which well-pair to include contributes to a more and more accurate mapping of the impermeable square area (from (b) through (f)).

For the quantitative evaluation of our algorithm, we define $S_{\cap}^{(k)}$ as the enclosed intersection area of arcs after adding k well pairs and we employ the following 3 metrics: a)

$$\alpha(k) = \frac{S_{\cap}^{(k)}}{S_{square}}; \text{ b) } \beta(k) = \frac{(S_{\cap}^{(k)}) \cap S_{square}}{S_{square}}; \text{ and c) } \gamma(k) = \frac{(S_{\cap}^{(k)}) \cap S_{square}}{S_{\cap}^{(k)}}.$$

The $\alpha(k)$ metric indicates the area mapping precision, i.e., how precise the arcs enclosed area, approximates the underground impermeable square area. It is more precise if $\alpha(k)$ is closer to 1. From Figure 7(a), we see clearly that as the number of well pairs increases, $\alpha(k)$ is getting closer to 1. Also Algorithm 1 performs better than the All Well-Pairs scheme as it decreases more quickly than the All Well-Pairs scheme.

The $\beta(k)$ metric indicates the location correctness, i.e., how precise the arcs enclosed area location approximate the underground impermeable square area location. It is more precise if $\beta(k)$ is closer to 1. From Figure 7(b), it is clear that as the number of well pairs increases, $\beta(k)$ for both scheme decrease. However, performance of Algorithm 1 is still better.

The $\gamma(k)$ metric indicates the efficiency of adding more well pairs. It is the ratio of the useful area over enclosed area. Algorithm 1 has better performance as shown in Figure 7(c).

6 CONCLUSIONS AND FUTURE WORK

In this paper, we investigate the problem of mapping underground impermeable areas using streamline approximations. We use arcs with the same lengths to approximate the shortest streamlines and compute the intersection of all arc pairs as our prediction of the impermeable region. Increasing the number of well pairs can increase the accuracy of the region mapping. We propose a perpendicular searching method to find the best well location for the next iteration so that the total number of wells employed is minimized.

The main limitation of our work is the solution space of our method. Since we are using the intersection of several arcs to characterize the shape and location of an impermeable region, our results can only be convex shapes. If the impermeable region is a concave shape, our solution will only obtain the convex hull of the unknown region. In this paper we are only using the distance between two adjacent nanodevices. If we employ the distance among non sequential nanodevices, we have the chance to reconstruct the shape of the streamline, which will make our mapping more accurate.

ACKNOWLEDGMENTS

This work was supported by NSF grant #1253968. We thank Mahima Suresh who contributed to the discussions of an early draft of this paper and the anonymous reviewers for their feedback.

REFERENCES

- [1] ABDOLLAH, E. Applications of nanotechnology in oil and gas industry. In *AIP Conference Proceedings* (December 2011).

- [2] AKKAS, M., AND SOKULLU, R. Wireless underground sensor networks: Channel modeling and operation analysis in the terahertz band. *International Journal of Antennas and Propagation* (2015).
- [3] AKKAS, M. A., ARKILDIZ, I. F., AND SOKULLU, R. Terahertz channel modeling of underground sensor networks in oil reservoirs. In *2012 IEEE Global Communications Conference (GLOBECOM)* (Dec 2012), pp. 543–548.
- [4] ARKILDIZ, I. F., JORNET, J. M., AND PIEROBON, M. Propagation models for nanocommunication networks. In *Proceedings of the Fourth European Conference on Antennas and Propagation* (April 2010), pp. 1–5.
- [5] BRITTO, P., AND SAGEEV, A. The effects of size, and orientation of an impermeable region on transient pressure testing. In *SPE California Regional Meeting* (Ventura, California, 1987).
- [6] CHOPRA, N. Characterisation of skin-based thz communication channel for nano-scale body-centric wireless networks.
- [7] CORDES, C., AND KINZELBACH, W. Continuous groundwater velocity fields and path lines in linear, bilinear, and trilinear finite elements. *Water Resources Research* 28 (1992), 2903–2911.
- [8] DATTA-GUPTA, A., AND KING, M. *Streamline Simulator*. Society of Petroleum Engineers, Richardson, Texas A&M University, 2005.
- [9] GONG, W., SURESH, M., SMITH, L., OSTFELD, A., AND STOLERU, R. Mobile sensor networks for optimal leak and backflow detection and localization in municipal water networks. *Environmental Modeling and Software* 80 (2016), 306–321.
- [10] GUO, H. *Enabling Wireless Communications in Complex Environments: From Underground and Underwater to Intra-body*. Dissertation/thesis, University at Buffalo, Buffalo, NY, April 2017.
- [11] IGOR, N., NIKOLAJ, Y., ALEKSANDR, P., AND MIKHAIL, A. Emerging petroleum-oriented nanotechnologies for reservoir engineering. In *Proceedings of the SPE Russian Oil and Gas Technical Conference and Exhibition* (Moscow, Russia, October 2006), Society of Petroleum Engineers.
- [12] JIMENEZ, E., SABIR, K., DATTA-GUPTA, A., AND KING, M. Spatial error and convergence in streamline simulation. *SPE Reservoir Evaluation & Engineering* 10, 3 (2007).
- [13] JU, B., AND DAI, S. A study of wettability and permeability change caused by adsorption of nanometer structured polysilicon on the surface of porous media. In *Proceedings of the SPE Asia Pacific Oil and Gas Conference and Exhibition* (Melbourne, Australia, October 2002), Society of Petroleum Engineers.
- [14] JU, B., AND FAN, T. Experimental study and mathematical model of nanoparticle transport in porous media. *Powder Technology* 192 (2009), 195–202.
- [15] JU, B., FAN, T., AND MA, M. Enhanced oil recovery by flooding with hydrophilic nanoparticles. *China Particology* 4 (2006), 41–46.
- [16] KONG, X., AND OHADI, M. Application of micro and nano technologies in the oil and gas industry—overview of recent progress. In *Proceedings of the SPE Abu Dhabi International Petroleum Exhibition and Conference* (Abu Dhabi, UAE, November 2010), Society of Petroleum Engineers.
- [17] NESTOR, M., AND HEBER, C. Detection of linear impermeable barriers by transient pressure analysis. In *SPE Conference Paper* (Utah, USA, 1983).
- [18] ORTIZ-LOPEZ, K. D., SURESH, M. A., AND STOLERU, R. Transmitters location optimization for drug delivery systems. In *Proceedings of the 5th ACM International Conference on Nanoscale Computing and Communication, NANOCOM 2018, Reykjavik, Iceland, September 05-07, 2018* (2018), pp. 26:1–26:6.
- [19] POLLOCK, D. Semi-analytical computation of path lines for finite-difference models. *Groundwaters* 26, 6 (1988), 743–750.
- [20] QUIREIN, J. A., GRABLE, J., CORNISH, B., STAMM, R., AND PERKINS, T. Micro-seismic fracture monitoring. In *SPWLA 47th Annual Logging Symposium* (Veracruz, Mexico, 2006), Society of Petrophysicists and Well-Log Analysis.
- [21] ROTHKOPF, B., FREDRICKSON, S., AND HERMANN, J. Case study: Merging modern reservoir characterization with traditional reservoir engineering. In *SPE Annual Technical Conference and Exhibition* (2003), Society of Petroleum Engineers.
- [22] S., B. Developments and challenges of mature oil fields. Tech. rep., Shell, October 2013.
- [23] SCHLUMBERGER. *ECLIPSE Industry-Reference Reservoir Simulator*, April 2019. <https://www.software.slb.com/products/eclipse>.
- [24] SØNDERGAARD, V. H., AND AUKEN, E. Integrated use of geophysics, drillings, logs and geochemistry in large scale groundwater mapping. In *SEG Annual Meeting* (2008), Society of Exploration Geophysicists.
- [25] SURESH, M., STOLERU, R., E.M., Z., AND SHIHADA, B. On event detection and localization in acyclic flow networks. *IEEE Transactions on Systems, Man, and Cybernetics: Systems* 43, 3 (2013).
- [26] WEIJERMARS, R., ZUO, L., AND WARREN, I. Modeling reservoir circulation and economic performance of the neal hot springs geothermal power plant (oregon, u.s.): An integrated case study. *Geothermics* 70 (2017), 155–172.
- [27] ZUO, L., LIM, J., CHEN, R., AND KING, M. Efficient calculation of flux conservative streamline trajectories on complex and unstructured grids. In *78th EAGE Conference and Exhibition* (Vienna, Austria, 2016).